The Henryk Niewodniczański
INSTITUTE OF NUCLEAR PHYSICS
Polish Academy of Sciences
ul. Radzikowskiego 152, 31-342 Kraków, Poland
www.ifj.edu.pl/publ/reports/2017/

Kraków, January 2017

Report No. 2097/AP

MECHANICAL ANALYSIS OF MIRROR PANELS USED IN CTA (CHERENKOV TELESCOPE ARRAY)

Jacek Błocki, Jerzy Michałowski, Przemysław Wąchal

Abstract

This paper presents results of numerical simulations of a three-layer rectangular plate and a rotationally symmetric plate, as well as panels of mirrors produced for the project Cherenkov Telescope Array - the CTA. Calculations were based on the finite element method and were prepared using ANSYS program. The problem of the three-layer rectangular plate and the rotationally symmetric plate loaded by bending moments on the edge was presented, with appropriate assumptions in the analysis. The theory of small and large deflections were analyzed and compared by the calculations. The curvature values at the middle and the end of plates were searched. Also bending moments needed to obtain the appropriate values of curvature were examined. Glass panels as a main part of CTA mirrors were described. The boundary conditions and loads, material properties were showed as well as the adopted assumptions in the analysis. Two cases were considered with two values of different radius of curvature. State of deformations and stresses which prevails in those parts of mirrors were checked. The results were depicted in the form of graphs of the radius of curvature and values of stresses for different values of mirror panel radius. Two methods, simple geometric and polynomial approximation, were used by which it was possible to approximate of radius of curvature changes in different places of panels after unloading the system.

1. Introduction

The international Cherenkov Telescope Array (CTA) project, that is, a network of Cherenkov telescopes, sets itself as one of the objectives the study of the Universe. With advent of his will considerably expand the range of the examined energy gamma radiation. The expected scope will be in the range of several tens [GeV] to over 100 [TeV] [1]. With advent of the twenty first century the development of the ground based observatory has accelerated and thus the ability to answer of the many questions which have asked by the many of scientist, has significantly increased. The international collaboration will be possess the very widely range more than 1000 scholars and researchers from all of the world, including: from Europe, North and South America and Asia. The assumption to build observatories in both hemispheres, will create an opportunity to observe the whole area of the sky. Constructing research instruments (telescopes) will pose to a challenge for the many engineers. One of its parts of this appliances will be the mirrors, which conception, design and manufacturing are complex, but very developmental process. Including numerical analysis which involving a different issues which are related to the mirror elements made the part of the complex design process.

2. Mirror for the Medium Size Telescope

The cold-slumped technique has been established and is being developed from several years. It was used including the production of the mirrors among others for the MAGIC II telescope [1]. The assumption during this process is that the panel consisting of two thin sheet of glass between which is a reinforcing layer with resin and reinforcement. The panel is shaped on the high precision mold by bending. The bending is caused by the negative pressure, between glass sheets and the mold. After the time in which the resin becomes enough hard the panel is taken off the mold.
This type of technique for the mirrors production is used at Institute of Nuclear Physics Polish Academy of Science in Krakow, Poland (IFJ PAN). Mirrors produced at IFJ PAN have a honeycomb structure. This mirror with its elements has shown in Fig.1.

Fig.1. Mirror produced at IFJ PAN, Krakow [2] (Copyright: Division of Scientific Equipment and Infrastructure Construction (DAI)).

Currently, the mirrors are being produced at IFJ PAN for the Medium Size Telescope (MST). These mirrors should be characterized by focal length f= 16,07 [m] and by curvature radius R_k which is equal to 32,14 [m]. The flat-to-flat dimension of the hexagonal mirror is equal to 1,2 [m]. In order to provide requirements defined by the CTA, the mirror surface is shaped on the high precision mold with vacuum and heating system. The whole structure consists of a rear panel and a front panel, which will have to reflect the radiation. The glass reflective layer is coated with of Al+SiO2 + Al + HfO2 + SiO2. Every individual panel is made by two sheets of glass with 2 [mm] thickness. Between this two sheets of glass there is a resin layer with the reinforcement in the form of fiberglass woven. Different configurations of glass sheets was considered, for example: float-float or Borofloat 33-Borofloat 33. The panels are merged together by spacers, which are aluminum pipes of constant diameter, thickness and height. To the rear panel are glued pads which allow to attach actuators to the mirror [2]. The presentation of a mirror structure was illustrated in Figure 2.

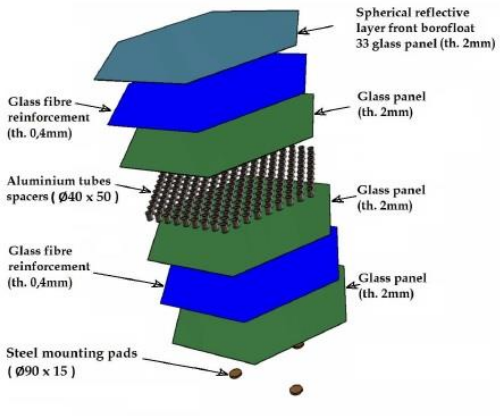

Fig.2. Mirror structure of the honeycomb [2].

3. The problem of bending three-layer plates

The analysis of CTA mirror panels was started from the problem of a rectangular plate and a rotationally symmetric plate loaded by bending moment at the edge. This approach was needed to determine and ascertain, whether it is necessary to use the large deflections assumption in further analyzes. The panel bending was performed to obtain a deflection w_{max} =0,006 [m]. The curvature in the middle and at the end of the plates were searched.

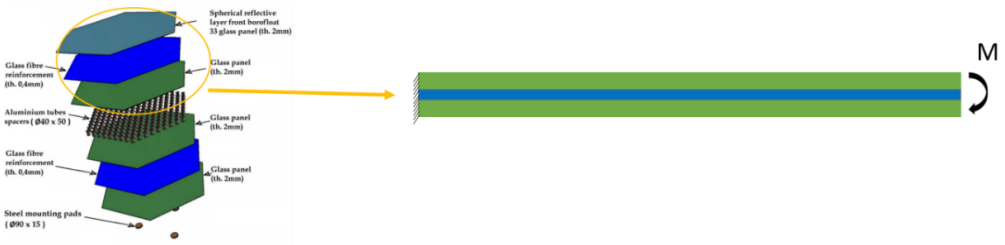

Fig.3. The three-layer plate model used in the numerical calculations (right) [3].

For small deflections the analytical calculations were done using equations (3.1) to (3.5). The exact description was done in [3], which shows the way to obtain w_{max} and R_k parameters. Results for the rectangular plate in Tab.2. were shown and for the rotationally symmetric plate in Tab.3. For large deflections results were obtained by numerical calculations using ANSYS program.
For the case of the rectangular plate, the equation for the maximum deflection value takes the following form [4]:

$$w_{max} = 0{,}125 \cdot \frac{M_o b^2}{D} \tag{3.1}$$

Where:

b – width of the whole plate [m],

M_o – moment intensity [Nm/m],

D – plate stiffness [Nm] given as:

$$D = \frac{Eh^3}{12(1-\upsilon^2)} \tag{3.2}$$

Where:

h – thickness of plate,

υ – Poisson's ratio,

E – Young modulus.

For the *l*=b/2 (in the middle of plate), eq. 3.1. takes form:

$$w_{max} = \frac{M_o l^2}{2D} \tag{3.3}$$

For the case with rotationally symmetric plate w_{max} was obtained as [5]:

$$w_{max} = \frac{M_o R^2}{2D(1+\upsilon)} \tag{3.4}$$

R – radius [m].

Then the curvature radius was obtained as:

$$R_k = \frac{D(1+\upsilon)}{M_o} \tag{3.5}$$

In ANSYS simulations the PLANE182, MESH200 and SHELL208 elements were used in the analysis. The PLANE182 elements were used to discretization of glass and resin layers. The SHELL208 elements were used only to allow to apply the bending moment on the edge of the plate. Additionally, MESH200 were used for lines discretization.

The plate consists of three layers, top, bottom and middle. Top and bottom layer have 2 [mm] thickness and middle has 0,3 [mm] thickness. It was assumed that the plate length is in one direction equal to 0,6 [m] and in the other its dimension is infinitive. For the rotationally case the plate radius is equal to 0,6 [m]. The choice of this dimensions was based on the actual dimensions of the single-panel mirror. As materials the construction glass and resin with reinforcement were used in the analysis. The material properties were shown in Tab.1.

Material	Properties	Value
Construction glass [6]	Young Modulus [GPa]	70
	Poisson's ratio [-]	0,2
Resin with reinforcement*	Young Modulus [GPa]	25
	Poisson's ratio [-]	0,23

Tab.1. The material properties used in the analysis .

*The property of resin together with reinforcement has been averaged.

The left edge of the rectangular plate has been fixed and right edge has been loaded by the bending moment. The boundary and loading conditions were shown in Fig.4a. and 4b. respectively [3].

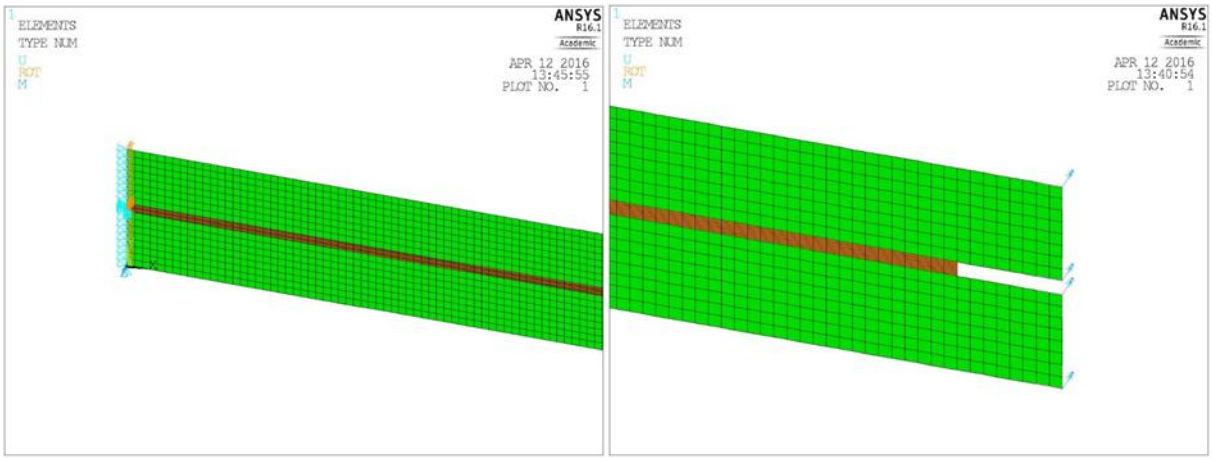

Fig.4. Boundary (4a) and loading (4b) conditions of three-layer plate.

3.1. Results

A comparison of obtained results from analytical and numerical calculations were done in tabular form. These results show difference between two approaches, that is assuming small and large deflections. The Moment intensity M_i (for rectangular plate) and the total moment M_t (for rotationally symmetric plate) were searched to obtain curvature radius R_k= 30 [m] using eq. (3.4.) and the numerical method.

Small deflection		
Bending moment intensity M_i $[\frac{Nm}{m}]$	3,3	
Length *l* [m]	0,3	0,6
Curvature κ [1/m]	0,0335	0,0335
Large deflection		
Bending moment intensity M_i $[\frac{Nm}{m}]$	5,3	
Length *l* [m]	0,3	0,6
Curvature κ [1/m]	0,0310	0,0334

Tab.2. Numerical results for the case with rectangular plate.

Small deflection		
Total bending moment M_t [Nm]	15	
Length *l* [m]	0,3	0,6
Curvature κ [1/m]	0,0342	0,0341
Large deflection		
Total bending moment M_t [Nm]	57	
Length *l* [m]	0,3	0,6
Curvature κ [1/m]	0,0167	0,0334

Tab.3. Numerical results for the case with rotationally symmetric plate.

For the case of a rectangular plate the obtained bending moment intensity M_i is greater (60%) for large deflections values than for small deflections. Additionally, the total bending moment value M_t for rotationally symmetric plate is nearly four times higher if we take into account large deflections than for the case where only small deflections are assumed.

Analyzing curvature values in the middle and at the end of the plate (Tab.2.) and (Tab.3.) [3] for small deflections, it can be seen that obtained values are the same. Compatibility can be seen in the both plates cases.

For large deflections, the values of curvature differ in the middle and at the end in the both cases. The results vary even by 50% for the rotationally symmetric plate. The main conclusion is that the large deflections has to be used.

4. Mirror panels

The main objective in this article are mirror panels which are being produced at IFJ PAN in Krakow for the MST. The manufacturing technology is being constantly developed and improved. The requirements which the mirror should meet are very high.
The structure of the mirror, which have been shown in Fig.2. consists of two panels:

- Rear, which has radius of curvature 22 [m];
- Front, which has radius of curvature 32,14 [m].

The different radius of curvature results from multistep production process (that is panel bending, gluing aluminum pipes to one of panels and so on). The final radius of curvature for the
panel with a reflective layer should have 32,14 [m]. The detailed description was presented in Chapter 2.
In this paper it will not be analyzed the whole mirror, but only panels with different radius of curvature. In performed analysis it has been taken to account two cases:

- The rear panel with radius of curvature 22 [m];
- The front panel with radius of curvature 32 [m].

In the following analysis, the rotationally symmetric character of the glass panels was assumed, that is, each panel has a circular shape with radius *R*= 0,6 [m]. This gives the benefits of the geometry simplification and reduction of time needed for numerical calculations. Each of the two glass layers has 2 [mm] thickness. The layer of resin and reinforcement has a 0,3 [mm] thickness. A part of the panel together with the division for the finite elements is shown in Fig.5.

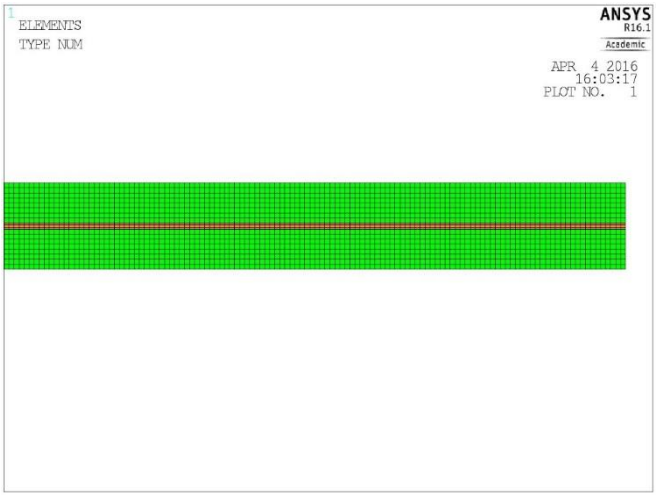

Fig.5. The finite element division of the panel used in numerical calculations [3].

The materials which have been used in this analysis are, as previously described in Chapter 3, construction glass and resin with reinforcement which has been presented in Table.1.
The location of used materials has been shown on Fig.6.

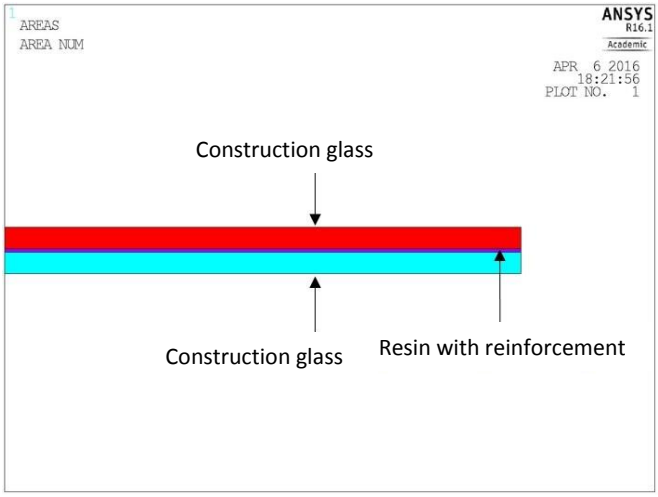

Fig.6. The materials used in the analysis [3].

Inasmuch as, the circular symmetry was assumed, the central line of the circular panel was fixed. The problem was reduced to two dimensions – Fig.7a. The pressure was applied to the upper and lower surface of the panel – Fig.7b.

In the real technological molding process the glass panels between which are liquid resin, are bent on the spherical mold under the action of atmospheric pressure. The process of forming the panel takes a predetermined amount of time in which the resin hardens. This technological process were simulated in the following way: in the first step, the mirror panel was loaded by the pressure p= 0,1 [MPa] applied to the upper and lower panel surface. The ANSYS approach of the birth and dead elements was applied to simulate the liquid resin, before and after its hardening, respectively.

In order to maintain distance between top and bottom glass layer which are independent from each other, during "freezing" the middle layer elements (simulated resin before hardening), two surfaces of contact elements (CONTA171) on bottom and top surface panels and appropriate TARGE169 elements have been generated. During the loading step, panel is pressed to mold (target elements). In the second step, middle layer elements were "unfreezing" which correspond to the moment when the resin has become hard. In the last step the applied pressure is gradually decreasing.

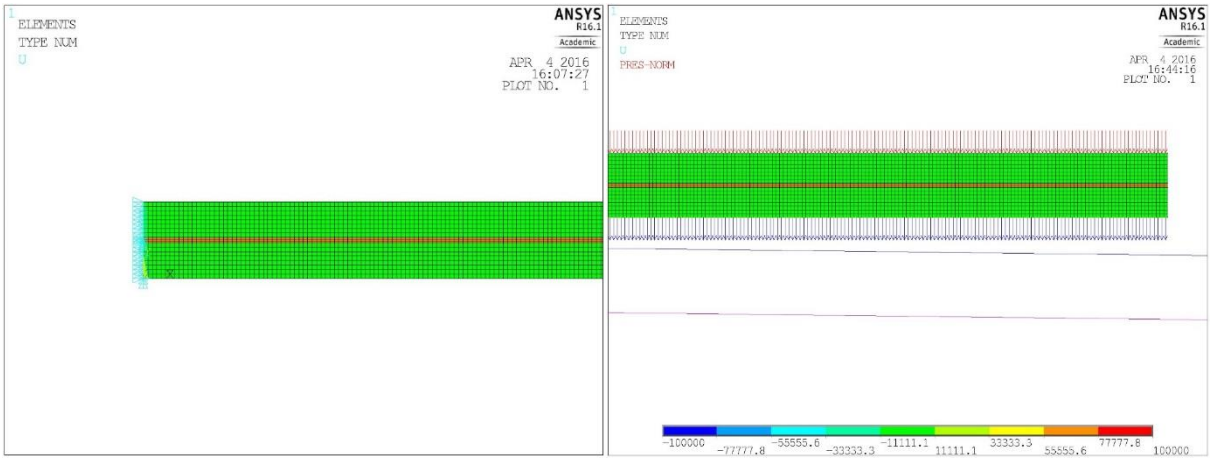

Fig.7. The boundary conditions (7a) and loading (7b) [3].

As before, different types of elements were used in this analysis which are shown in Fig.8a. and 8b. and listed below:

- PLANE182 – amount 45600 (the total number of elements),
- MESH200 – 9600,
- TARGE169 – 2,
- CONTA171 – 4800.

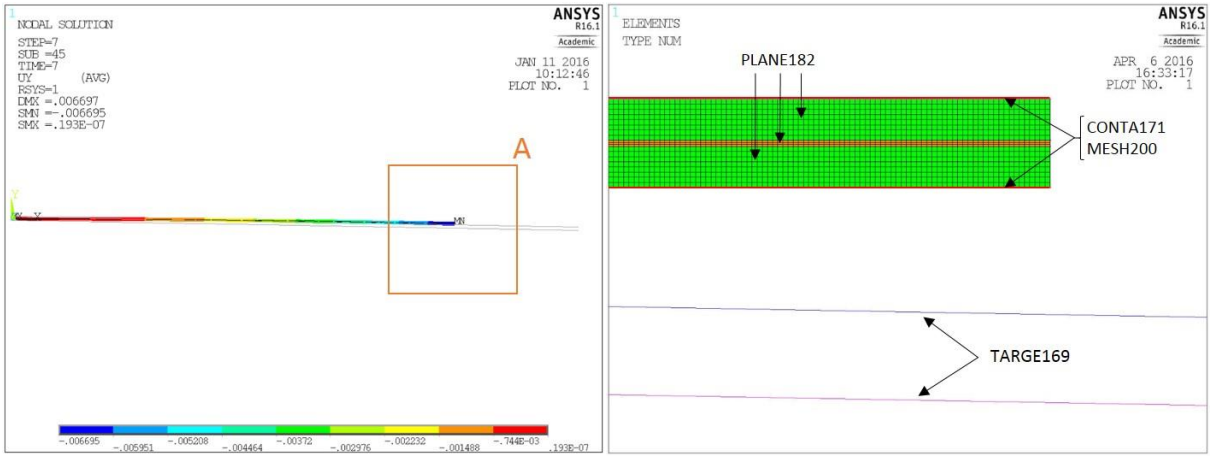

Fig.8. Model (8a) and elements used in the analysis – detail A (8b) [3].

4.1. Results

4.1.1. Radius of curvature

After unloading the radius of curvature R_k on the bottom surface where a reflective layer is located has been checked. This parameter was chosen, because maintain its constant value, along whole panel's radius of curvature, can affect of its quality. Values of R_k have been calculated in two ways. In the first method (Method I) the following formulas has been used:

$$R_k = \frac{1}{2}\left(c + \frac{e^2}{c}\right) \tag{4.1}$$

Where *c* and *e* are shown in Fig.9;
We have:

$$c = u_z \text{ and } e = (P_r + u_r) \tag{4.2a, 4.2b}$$

where:
u_z – value of displacement in axial direction, [m];
P_r – radial coordinate of node;
u_r – value of displacement in r direction, [m].

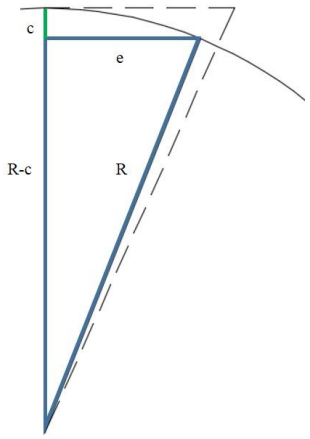

Fig.9. Geometrical relationship [3].

In the second method (the Method II) the radius of curvature R_k is calculated from following formulas:

$$R_k = \frac{[1+(Q'_m(u))^2]^{\frac{3}{2}}}{|Q''_m(u)|} \tag{4.3}$$

where $Q_m(u)$ Gram polynomials [7].

These polynomials are defined as a system of $\varphi_0(x)$,$\varphi_1(x)$,…,$\varphi_m(x)$ orthonormal functions with weight function $y=w(x)\equiv 1$ on a set $X=\{x_0, x_1,\ldots, x_n\}$ when:

$$(\varphi_j , \varphi_k)=\sum_{i=0}^{n} w(x_i)\varphi_j (x_i)\varphi_k (x_i) = \sum_{i=0}^{n} \varphi_j (x_i)\varphi_k (x_i), \tag{4.4}$$

0 for j≠k and 1 for j=k.

It is assumed that points of approximated function are taken from deformed shape of the panels and marked by u_0, u_1, …, u_n, as points of segment [-1,1] with *n* equidistant sections $u_i = \frac{2_i}{n} - 1$ for i= 0, 1, …, 6.

Recurrence relationships are described as:

$$G_{-1}(u) = 0, \quad G_0(u) = \alpha_0 = \frac{1}{\sqrt{(n+1)}}, G_k(u) = \alpha_k u G_{k-1}(u) - \gamma_k G_{k-2}(u) \tag{4.5a, 4.5b, 4.5c}$$

for k=1, 2,…,5.

and:

$$\alpha_k = \frac{n}{k}\sqrt{\frac{4k^2-1}{(n+1)^2-k^2}}, \qquad \gamma_k = \frac{\alpha_k}{\alpha_k - 1} \tag{4.6a, 4.6b}$$

for k=1,2,…5,

where α_k and γ_k are the ancillary variables.

The $Q_m(u)$ are defined by:

$$Q_m(u) = a_0 G_0(u) + a_1 G_1(u) + , \ldots , + a_m G_m(u) \tag{4.7}$$

for m ≤ n-1, with weight function $y=w(x)\equiv 1$ on a set $X=\{u_0, u_1,\ldots, u_n\}$, to approximate the function $y=f(x)$ for [-1,1].

Presented here all numerical calculations have been done for two kinds of panels: with 22 [m] and 32 [m] radius of curvature. Results for both cases were showed in Fig.10. and 11 [3].

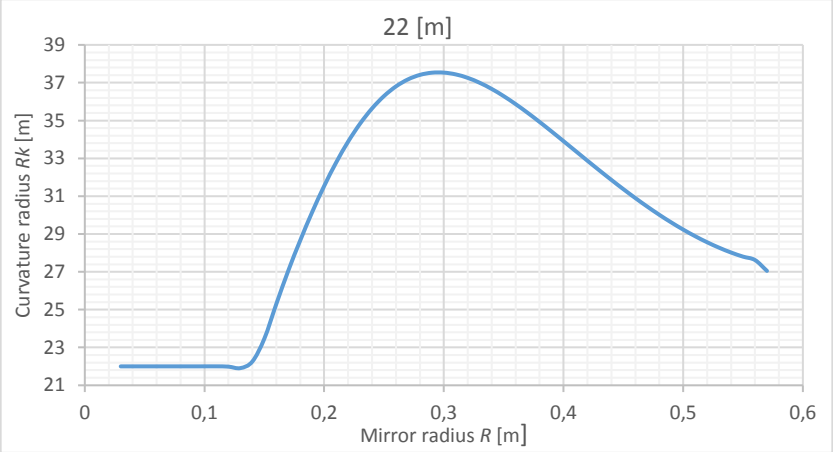

Fig.10. The radius of curvature after unloading for R_k=22[m].

For the case of the panel with the initial radius of curvature R_{kp}= 22 [m], by use of the Method II, there are shown in Fig.10 radius of curvature changes, which are not noticeable when using the Method I (see [3]). Unchangeable radius of curvature values, can be seen in the certain range. The maximum deviation of the radius between its initial and final value is about 15,5 [m]. Maximum value occurs in the middle of radius panel for R= 0,3 [m].

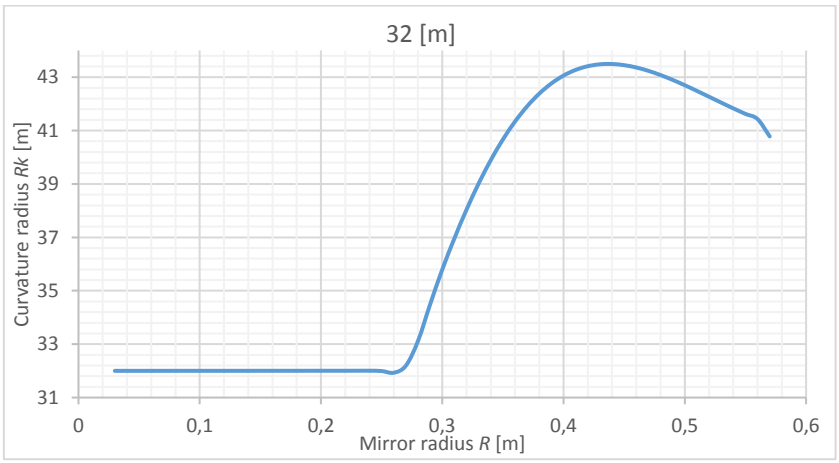

Fig.11. The radius of curvature after unloading for R_k=32[m].

By use of the Method II we can notice that radius of curvature changes for case R_{kp}= 32 [m] (Fig.11.), have different course than for R_{kp}= 22 [m]. Maximum value R_k= 43,5 [m] is not occur in the middle of

the panel, as occurred for the smaller initial radius R_{kp}. The range of constant radius of curvature which has been preserved is two times greater, than for panel with R_{kp}= 22 [m].

4.1.2. Deflection

Deflections, which arise during shaping the panels were analyzed. This deflections have been compared with curves which describe ideal sphere (R=22 [m] and 32 [m]), respectively. Aim of such interpretation was verification whether the structure after shaping behaves in a correct and predictable way. In this paper the results of deflections for the panel with the radius of curvature equal to 22 [m] have been presented in Fig.12. The rest of results have been presented in [3].

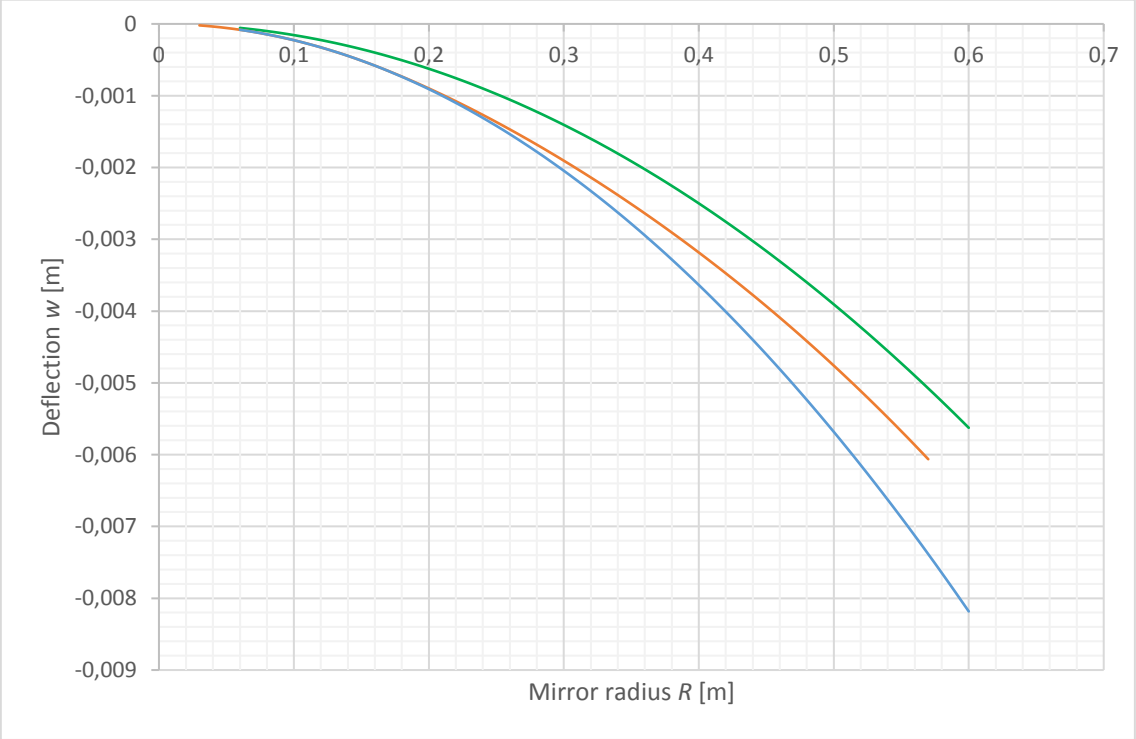

Fig.12. Comparison of deflection for case R_{kp}= 22 [m].

The blue and green lines are showing the ideal curves with constant radius of curvatures equal to 22 [m] and 32 [m], respectively. The deflection of the panel (R_{kp}= 22 [m]) obtained from the calculations (orange line) for coincides with the ideal sphere having a radius of curvature of 22 [m], but only in a certain range. In this range the radius of curvature is constant (Fig.10.).

4.1.3. Stresses

After system unloading for mirror panels with two different initial radius of curvature, stress state analysis was also done. The places where stresses were examined, were bottom surface in bottom glass layer (compressed surface) and top surface in top glass layer (tensile surface) along mirror panel radius *R*. Stresses was examined in three directions: radial σ_r, circumferential σ_φ, axial σ_z and reduced stresses according to Huber-Mises-Hencky'ego hypothesis σ_{HMH}.

In this paper results for circumferential stress σ_φ was showed for the case with radius of curvature equal to 22 [m] on the compression side, and the tension side. All of others stress cases in diagram form was depicted in [3].

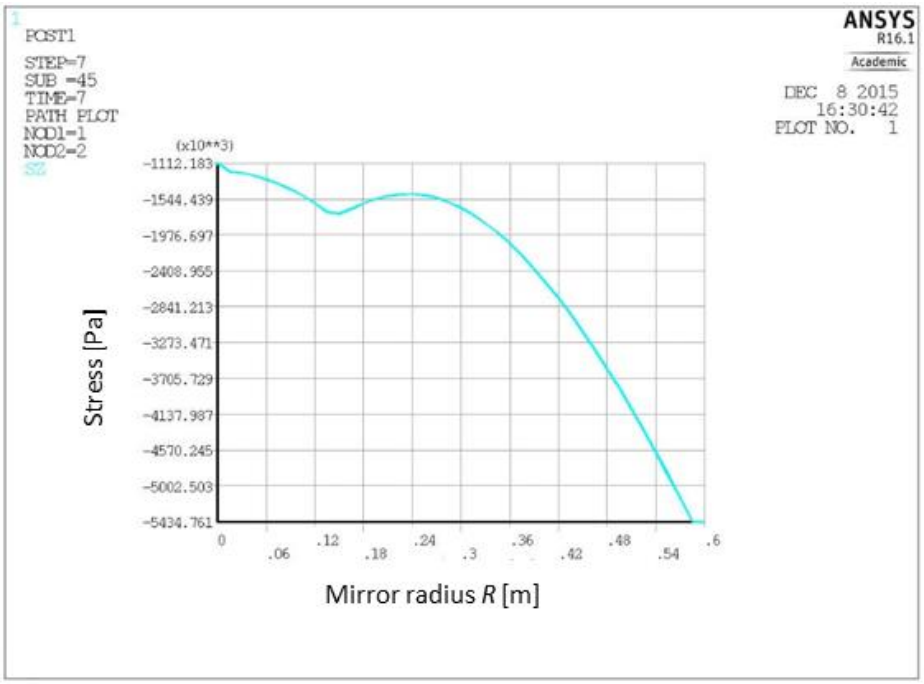

Fig.13. Circumferential stress σ_φ at compressed side.

For the case with circumferential stress σ_φ showed in Fig.13., it can be seen, that in the whole range of mirror radius *R,* the values are negative, which indicates that, in the circumferential direction compression occurs. The minimum circumferential stress value is equal σ_φ= -5,43 [MPa] and there are near the right mirror edge.

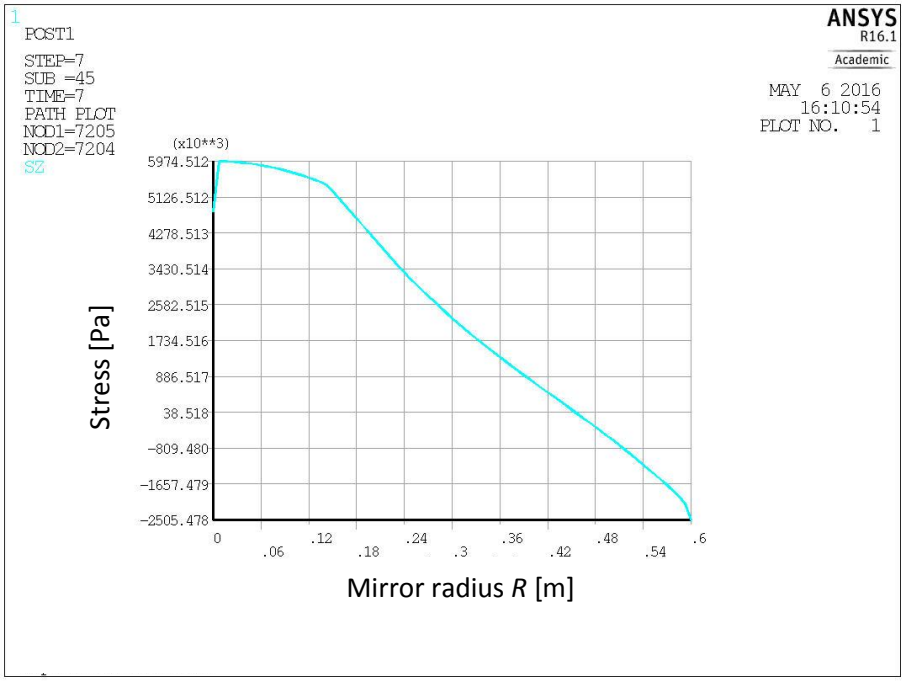

Fig.14. Circumferential stress σ_φ at tensile side.

Circumferential stress σ_φ depicted in Fig.14. reaches the maximum value close to the center of the panel. The maximum value is equal to 6 [MPa]. In the small range (for *R*=0,5÷0,6 [m]) stresses have negative value, what means that top surface is as well compressed.

The maximum stress values in panels, are shown in Tab. 4 and Tab.5.

Maximum stress value [MPa]	Initial radius of curvature R_{kp}= 22 [m]	Initial radius of curvature R_{kp}= 32 [m]
Radial stress σ_r	-1,86	-1,31
Circumferential stress σ_φ	-5,43	-4,11
Axial stress σ_z	0,22	0,15
Reduced stress σ_{HMH}	5,50	4,17

Tab.4. Maximum stress values at compressed panel side.

Maximum stress value [MPa]	Initial radius of curvature R_{kp}= 22 [m]	Initial radius of curvature R_{kp}= 32 [m]
Radial stress σ_r	5,90	3,87
Circumferential stress σ_φ	6,00	3,90
Axial stress σ_z	-0,21	-0,15
Reduced stress σ_{HMH}	6,20	4,10

Tab.5. Maximum stress values at extended panel side.

After analyzing the stress state it can be ascertain, that the maximum compressing stress values at compressed side – Tab.4. are far away from the allowable stress for compression for glass (σ_{maxc}= 1000 [MPa][8]).
In case of the top glass layer – Tab.5. also stress values do not exceed the allowable stress for bending (σ_{maxr}= 45 [MPa][8]).
To sum up, in the panels consist of two glued glass sheets the extreme value of stresses does not exceed the allowable stress.

5. Conclusions

The following conclusions can be drawn:

- the large deflection has to be included in the bending analysis of the glass panels,
- two methods were used in the analysis: of the final radius of curvature Method I which consists in geometrical dependences and Method II which includes a fifth stage orthonormal polynomial approximation,
- the deflections obtained from numerical calculations are not in contradiction with the shape of the ideal sphere,
- the extreme value of stresses caused by the panels bending does not exceed the allowable stresses.

References:

[1] The CTA Consortium: *Design concepts for the Cherenkov Telescope Array CTA: an advanced facility for ground-based high-energy gamma-ray astronomy,* Exp Astron, 32, 2011.

[2] Michałowski J., Dyrda M., Niemiec J., Sowiński M., Stodulski M.: *Developments of a new mirror technology for the Cherenkov Telescope Array,* Proceedings of Science, 988, 2015.

[3] Wąchal P.: Analiza mechaniczna zwierciadeł wykorzystywanych w CTA (Cherenkov Telescope Array), Praca magisterska, Politechnika Krakowska, 2016.

[4] Timoshenko S., Woinowsky-Krieger S.: *Teoria płyt i powłok*, Wydawnictwo Arkady, Warszawa 1962.

[5] Niezgodziński M. E., Niezgodziński T.: *Wzory, wykresy i tablice wytrzymałościowe,* Wydawnictwo Naukowo-Techniczne, Warszawa 2013.

[6] PN-EN 572-1:2005.

[7] Wykłady Politechnika Gdańska, Wydział Elektroniki, Telekomunikacji i Informatyki, *http://eti.pg.edu.pl/documents/176593/26763380/Wykl_AlgorOblicz_3.pdf*, [Available on 04.01.2017].

[8] http://oknotest.pl/szyby-i-szklo/szklo, [Available on 04.01.2017].